HHS Public Access

Author manuscript

ACS Appl Mater Interfaces. Author manuscript; available in PMC 2018 March 29.

Published in final edited form as:

ACS Appl Mater Interfaces. 2017 March 29; 9(12): 10494–10503. doi:10.1021/acsami.7b00221.

In Situ-Forming Polyamidoamine Dendrimer Hydrogels with Tunable Properties Prepared via Aza-Michael Addition Reaction

Juan Wang[1], **Hongliang He**[1], **Remy Cooper**[2], and **Hu Yang**[1,3,4,*]

[1]Department of Chemical and Life Science Engineering, Virginia Commonwealth University, Richmond, Virginia 23219, United States

[2]Department of Biomedical Engineering, Virginia Commonwealth University, Richmond, Virginia 23284, United States

[3]Department of Pharmaceutics, Virginia Commonwealth University, Richmond, Virginia 23298, United States

[4]Massey Cancer Center, Virginia Commonwealth University, Richmond, Virginia 23298, United States

Abstract

In this work, we describe synthesis and characterization of novel *in situ*-forming polyamidoamine (PAMAM) dendrimer hydrogels (DHs) with tunable properties prepared via highly efficient aza-Michael addition reaction. The nucleophilic amines on the dendrimer surface reacted with α, β-unsaturated ester in acrylate groups of polyethylene glycol diacrylate (PEG DA, MW=575 g/mol) via aza-Michael addition reaction to form dendrimer hydrogels without catalyst. The solidification time, rheological behavior, network structure, swelling and degradation properties of the hydrogel were tuned by adjusting dendrimer surface acetylation degree and dendrimer concentration. The DHs were shown to be highly cytocompatible and support cell adhesion and proliferation. We also prepared an injectable dendrimer hydrogel formulation to deliver anticancer drug 5-FU and demonstrated that the injectable formulation efficiently inhibited tumor growth following intratumoral injection. Taken together, this new class of dendrimer hydrogel prepared by aza-Michael addition reaction can serve as a safe tunable platform for drug delivery and tissue engineering.

Keywords

dendrimer; injectable hydrogel; click chemistry; in situ forming; localized chemotherapy

*To whom correspondence should be addressed: hyang2@vcu.edu.

SUPPORTING INFORMATION

HPLC analysis of acetylated G5, amplitude sweep of DH-G5-Ac^{X}-5%, SEM images and hydrogel photos of DH-G5-Ac^{X}-5%, DH-G5-Ac^{X}-10%, and DH-G5-Ac^{X}-20%, quantification of NIH 3T3 cells on TCPS and DH-G5-Ac^{64}-10%, and cytotoxicity assay of DH-G5-Ac^{64}-10%.

INTRODUCTION

There is an ongoing interest developing hydrogels with *in situ* formability for biomedical applications. In contrast to pre-formed hydrogels, *in situ* forming-hydrogels maintain fluidity during administration and form gel rapidly *in situ* at the injection site.[1] Drugs, proteins, bioactive molecules and even cells can be readily packaged into injectable hydrogels.[2–13] Injectable hydrogels can be prepared by using a variety of chemical methods such as photoinitiated cross-linking reactions,[14–15] click chemistry,[16–20] Schiff's base reaction,[21–23] and enzyme-catalyzed reactions.[24–27] Physical methods utilizing non-covalent intermolecular interactions such as hydrophobic interactions,[28] electrostatic interactions, [29–30] and host-guest interactions [31–32] have also been explored to make injectable hydrogels. Using dendrimers as building blocks to form hydrogels have been recently explored by us and other groups.[33–40] Dendrimer hydrogels are attractive by virtue of high flexibility in delivering drugs of different types.[41–44]

Herein, we report on injectable *in situ*-forming polyamidoamine (PAMAM) dendrimer hydrogels using highly efficient aza-Michael addition reaction. The aza-Michael addition reaction is efficient in coupling nitrogen nucleophiles to α,β-unsaturated carbonyl compounds. We adopted the aza-Michael addition reaction to construct injectable dendrimer hydrogels by reacting PAMAM dendrimers carrying primary surface amines to polyethylene glycol diacrylate (PEG-DA). It is the strong nucleophilicity of primary amines that enables the reaction to proceed in aqueous solutions without using base catalysts. The combination of the dendritic structure of PAMAM dendrimer and the efficient aza-Michael addition yields unique *in situ* forming dendrimer hydrogels. The high degree of functionality of PAMAM dendrimer offers a convenient way to modulate dendrimer hydrogel properties. We chose PAMAM dendrimer G5 as the underlying core and tuned its surface charges via various degrees of acetylation using acetic anhydride. We systematically investigated *in situ* gelling kinetics, network structures and swelling kinetics of the dendrimer hydrogels prepared using aza-Michael addition reaction of G5 and acetylated G5 with short-chain PEG DA (M_n=575 g/mol). The biocompatibility and the ability of the forming dendrimer hydrogels to support cell adhesion were also studied. One potential application of injectable dendrimer hydrogels is localized anticancer drug delivery. Anticancer drugs can be highly localized to attack tumor cells more directly while avoiding systemic toxicity effects. Intratumoral formulation of injectable dendrimer hydrogel loaded with fluorouracil (5-FU) was tested in a xenograft mouse model of head and neck cancer.

MATERIALS AND METHODS

Materials

EDA-core PAMAM dendrimer generation 5 (G5) was purchased from Dendritech (Midland, MI). Polyethylene glycol diacrylate (PEG-DA, M_n = 575 g/mol), acetic anhydride (Ac, 98.0%), triethylamine (TEA, 99%), 4′,6-diamidino-2-phenylindole (DAPI), fluorouracil (5-FU) and fluorescein 5(6)-isothiocyanate (FITC) were purchased from Sigma-Aldrich.

Synthesis and Characterization of Acetylated G5

Synthesis—Acetylated PAMAM dendrimers were synthesized following the reported procedures.[45–46] Briefly, PAMAM dendrimer G5 (288 mg, 0.01 mmol) in 10 mL of methanol was mixed with various amounts of Ac in the presence of TEA (Table 1). After 12 h, the reaction mixtures were dialyzed in pH 8 sodium bicarbonate buffer and then in deionized water using SnakeSkin dialysis tubing (3.5K MWCO). After lyophilization, G5-Ac$^{\#}$ conjugates (# indicates an average of Ac per dendrimer determined by ^{1}H NMR) were obtained. FITC-labeled G5 and G5-Ac were also prepared following the protocol described previously.[47]

Proton Nuclear Magnetic Resonance (^{1}H NMR) Spectroscopy—^{1}H NMR spectra of acetylated PAMAM dendrimers were obtained on a Bruker AV-III 400 MHz or a Bruker 600 MHz spectrometer. The degrees of acetylation were calculated based on the ratio of the integrals for methyl protons of acetyl groups to the dendrimer protons.

High Performance Liquid Chromatography (HPLC)—The purity of acetylated G5 was determined by using a HPLC (Waters) system equipped with a Waters 1515 isocratic HPLC pump, a Waters 2487 dual λ absorbance detector and a Waters 717 plus autosampler. The mobile phase was the mixture of acetonitrile and water (acetonitrile/water = 3/1 by volume). The eluents were monitored by the UV detector at 220 nm and 360 nm.

Zeta Potential—The zeta potentials of the acetylated PAMAM dendrimers were characterized by using Malvern Zetasizer Nano ZS90 (Malvern Instruments, Worcestershire, U.K.).

Preparation and Characterization of Dendrimer Hydrogels

Formulations—PAMAM dendrimer (G5, G5-Ac^{64}, G5-Ac^{90}, or G5-Ac^{106}) was dissolved in deionized water or pH 7.4 PBS at 25 °C to have various concentrations (5, 10, or 20 wt. %). Appropriate amounts of PEG-DA 575 were added to maintain an equal molar ratio of acrylate to dendrimer surface primary amines in the solution. DH-G5-Ac^{x}-#% denotes dendrimer hydrogel where x is the number of the acetyl groups and #% is the weight percentage of G5-Ac^{x} in solution. DH-G5-#% dendrimer hydrogels were also prepared at various concentrations. Inverted test tube method was applied to estimate dendrimer hydrogel solidification time, at which the gel does not flow in 30 s after the test tube is inverted. In this work, we tested hydrogel solidification time up to 100 min.

Scanning Electron Microscopy (SEM)—Lyophilized dendrimer hydrogel samples were coated with platinum for 90 seconds using an ion sputter. SEM images were taken under a scanning electron microscopy JEOL LV-5610.

Rheological Measurements—Rheological measurements were carried out on Discovery hybrid rheometer HR-3 (TA Instruments) and a 20 mm parallel plate geometry was used. Measurements were obtained at 25 °C, which was achieved via a water bath and a temperature-controlled Peltier plate. A small-amplitude dynamic oscillatory time sweep was conducted to examine the evolution of storage modulus (G′) and loss modulus (G″) and

determine the sol-to-gel transition of the hydrogel solutions. During the small-amplitude dynamic oscillatory time sweep, the angular frequency was set to be 1 rad/s and the strain was kept constant as 1%. To conduct oscillatory frequency sweeps, an amplitude sweep (G′, G″ *vs* strain) was performed first to determine a linear viscoelastic region. Within the linear viscoelastic region, oscillatory frequency sweeps were then carried out under a constant strain of 1% in the frequency range of 0.1–10 rad/s.

Swelling Studies—Water absorption kinetics of dendrimer hydrogels (DH-G5-20%, DH-G5-Ac^{64}-20%, and DH-G5-Ac^{90}-20%) was determined. Each lyophilized hydrogel was immersed and incubated in 1 mL of PBS (pH = 7.4) at 37 °C. The supernatant was gently sucked out at different time intervals and the swollen hydrogel sample was weighed. The measurement period was up to 12 h in order to reach the maximum absorption. The swelling ratio (%) = $(W_t - W_0)/W_0 \times 100$, where W_t represents the mass of the swollen sample and W_0 represents the initial mass of the dry sample.

Disintegration Studies—The disintegration properties of dendrimer hydrogels (DH-G5-20%, DH-G5-Ac^{64}-20%, DH-G5-Ac^{90}-20%, and DH-G5-Ac^{106}-20%) was determined at 37 °C. Each lyophilized hydrogel was weighted and incubated at 37 °C in 1.5 mL-centrifuge tubes containing 500 μL of PBS (pH = 7.4). After 6 h, 24 h, and 48 h, respectively, the samples were centrifuged and the sample residues were freeze-dried and weighed. The disintegration was calculated based on the following formula: disintegration (%) = $(W_{d0} - W_{dt})/W_{d0} \times 100$ where W_{dt} represents the mass of the freeze-dried sample after incubation and W_{d0} represents the initial mass of the dry sample.

Cell Adhesion Studies

To examine whether dendrimer hydrogel supports cell attachment, 2.5 μL/well of FITC labeled dendrimer hydrogel DH-G5(FITC)-Ac^{64}-10% was added to the 96-well plate and shaken for 24 h to form a thin layer of DH at the bottom of the well. NIH3T3 cells were then seeded on the hydrogel with a density of 1×10^4 cell/well. After 24 h and 48 h, respectively, the cell culture medium was removed and the cells were fixed and stained with DAPI and imaged under a fluorescence microscope (Nikon Eclipse *Ti*) under DAPI and FITC channels. A control experiment without DH was carried out by seeding cells directly on the tissue culture polystyrene plate (TCPS). In addition, to prove the stability of DH during the cell attachment and growth, three letters ‘VCU’ were written with DH-G5(FITC)-Ac^{64}-10% and incubated in the culture medium at 37 °C for either 24 h or 48 h. The letters were imaged to monitor the stability of the hydrogel. Cell viability after 24 h and 48 h-culture on the hydrogel was independently determined by using WST-1 assay.

Liquid Dendrimer Hydrogel Loaded with 5-FU

A liquid dendrimer hydrogel, i.e., DH-G5-0.5% was used to load anticancer drug 5-FU and the formulation was examined for drug delivery *in vitro* and *in vivo*.

In Vitro Drug Release Kinetics—Drug release was performed on 5-FU loaded into DH-G5-0.5% (5-FU/DH-G5-0.5%). Briefly, Free 5-FU (300 μg) in PBS or DH-G5-0.5% containing 300 μg of 5-FU was transferred to dialysis bags (MWCO = 500–1000 Da) and

suspended in 30 mL of PBS in 50-mL centrifuge tubes. The tubes were maintained at 37 °C. At predetermined time intervals up to 24 h, 1 mL of medium outside the dialysis bag was withdrawn, and the amount of drug released into the medium was analyzed on HPLC against a standard curve of 5-FU. After each sampling, 1 mL of fresh PBS was added to maintain a constant volume and sink condition. All experiments were performed in triplicate.

Cytotoxicity Assessment—To study the cytocompatibility of DH-G5-0.5%, NIH3T3 fibroblasts were seeded in a 96-well plate at a density of 1×10^4 cell/well. After 24 h of cell attachment, the culture medium was replaced by 200 μL of medium containing DH-G5-0.5% at different concentrations. Cell viability after 24 h-and 48 h-incubation was determined by using WST-1 assay.

In Vivo Formulation Toxicity and Drug Efficacy Studies—Female athymic nude mice (4–6 weeks-old, 18–20 g, Harlan Sprague–Dawley, Indianapolis, IN) were used in the study. HN12 head and neck cancerous cells (5×10^6 cells/ml) in 200 μL of PBS were injected into the dorsal subcutaneous tissue of host mice to induce tumor xenografts. Two weeks later, the tumor-bearing mice were divided into four groups of three to receive intratumoral injection of PBS, DH-G5-0.5%, 5-FU/PBS, or 5-FU/DH-G5-0.5%. Injection solution volume was 2.5 mL/kg, and 5-FU dose was 5 mg/kg for the first injection and then 10 mg/kg at later time points. Tumor volume and body weight of tumor-bearing mice were monitored throughout the experiment. Tumor volume (V_t) was calculated with the formula: $V_t = \text{width}^2\times\text{length}/2$. Relative tumor volume at different time point was calculated by normalized to the initial tumor volume: Relative tumor volume = V_t/V_0, where V_0 represents the initial tumor volume. At the end of experiment, the mice were euthanized and tumors were dissected out for hematoxylin and eosin (H&E) staining. The animal experiments were approved by the Institutional Animal Care and Use Committee of Virginia Commonwealth University.

Statistical Analysis

The data were analyzed by using unpaired t-test and one way analysis of variance (ANOVA). *P* values less than 0.05 were considered statistically significant.

RESULTS AND DISCUSSION

Acetylation of G5

The aza-Michael addition reaction is one of the most exploited reactions to form carbon–nitrogen bonds in organic chemistry. Full generation PAMAM dendrimers contain numerous primary amines on the surface and secondary amines in the core. These strong nucleophilic amines present in the dendrimer backbone can react with α, β-unsaturated ester in acrylate group of PEG DA via aza-Michael addition reaction to form a cross-linked network. Despite the fact that original secondary amines are more reactive than primary amines in the aza-Michael addition reaction,[48] their availability to the reaction is low due to steric hindrance. Therefore, the reaction predominantly utilizes the primary amines on the dendrimer surface. Converting surface amines to non-reactive acetyl groups provides a means to modulate reaction kinetics and cross-linked network. To this end, G5-Ac conjugates with various

degrees of acetylation were synthesized. The purity of the acetylated PAMAM dendrimers was verified with the HPLC analysis (Figure S1). The ^{1}H NMR spectra confirm the presence of the methyl protons of the conjugated acetyl groups at 1.96 ppm and the peak intensity increases with increasing degree of acetylation (Figure 1A). Based on the integrals of methyl protons of acetyl groups to the dendrimer protons (peaks at 3.28, 2.80, 2.61, and 2.39 ppm), an average of 64, 90, and 106 acetyl groups were coupled to the dendrimer, respectively. Unmodified PAMAM G5 has a zeta potential of 50.03 mV.[49] The zeta potential of G5-Ac conjugates decreases with increasing acetylation degree, but all remain positive (Figure 1B). Since PAMAM dendrimer G5 surface property was altered by converting primary amines into acetyl groups, G5 functionalized with different degrees of acetylation were utilized to modulate in situ gelation kinetics of dendrimer hydrogels.

Tunable Hydrogel Solidification

The aza-Michael addition reaction of G5 or G5-Ac with PEG-DA occurred at room temperature in the absence of any other reagents. An inverted test tube method (Figure S3 and Figure S4) was applied to detect the flow properties of the hydrogels and estimate solidification time. To study aza-Michael addition reactions of dendrimer and PEG DA under relatively controllable conditions, we chose degree of acetylation and dendrimer concentration as primary variables and kept equal molar quantities of dendrimer primary amines and PEG acrylate groups in the reactions. The aza-Michael addition reaction was able to proceed under the conditions studied. As shown in Figure 2, both degree of acetylation and dendrimer concentration affect solidification kinetics. However, not all of dendrimer hydrogels underwent sol-gel phase transition to solidify. Those having high degrees of acetylation either only formed liquid hydrogels or required much longer time to solidify at low concentrations. They were not included in the figure. Within the observation time window, DH-G5-Ac^{90} solidified at 10 and 20 wt%. But DH-G5-Ac^{106} solidified only at 20 wt%. In contrast, lower degree of acetylation and higher dendrimer concentration enable dendrimer hydrogels to solidify more rapidly. At 20%, DH-G5, DH-G5-Ac^{64}, DH-G5-Ac^{90} and DH-G5-Ac^{106} were able to solidify. Solidification times were 1 min, 4 min, 146 min, and 158 min, respectively. Both DH-G5 and DH-G5-Ac^{64} solidified at even lower concentrations at 5 wt% and 10 wt% but took longer time. For instance, solidification time of DH-G5 at 10 wt% was 2.5 min and was further extended to 11 min when the concentration was reduced to 5 wt%.

Effect of Acetylation on Swelling and Disintegration Behaviors

Given that DH-G5 and DH-G5-Ac regardless of degree of acetylation were able to solidify at 20 wt%, we examined their morphologies and the effect of degree of acetylation on hydrogel swelling and disintegration. As shown in Figure 3A, dendrimers with more amine groups tended to form more compact hydrogels with rough microstructures while those with less amine groups showing a loose and smooth structure. The formation of dense microstructures is attributed to the high density of cross-linking sites. Their swelling behaviors were examined in pH 7.4 PBS at 37 °C. The swelling kinetics of DH-G5-Ac^{106}-20% was not obtained as it was unstable and started to disintegrate after 6 h. As for DH-G5-20%, DH-G5-Ac^{64}-20% and DH-G5-Ac^{90}-20%, the dehydrated samples showed a

rapid swelling rate in the first 0.25 h and absorbed 107%, 259%, and 182% of its own weight of PBS, respectively. The swelling then gradually reached equilibrium (Figure 3B).

Interestingly, the swelling rate of DH-G5-20% was significantly lower than the other two DHs. It took DH-G5-20% 6 h to reach its equilibrium, ~240%, while it took DH-G5-Ac^{64}-20% and DH-G5-Ac^{90}-20% only 2 h to reach equilibrium swelling ratios (~326% for DH-G5-Ac^{64}-20% and 250% for DH-G5-Ac^{90}-20%). In addition, DH-G5-Ac^{64}-20% and DH-G5-Ac^{90}-20% exhibited the highest and lowest equilibrium swelling ratio, respectively. The different swelling ratios and rates may be attributed to the 3-D cross-linked structures of the hydrogel. Generally speaking, a loose cross-linked network allows more PBS to be absorbed into the swollen hydrogel, and at the same time the swelling rate would be higher. This explains why the equilibrium swelling ratio of DH-G5-Ac^{64}-20% is higher than that of DH-G5-20% and why DH-G5-20% has the lowest swelling rate. As for DH-G5-Ac^{90}-20%, the most loosely cross-linked structure is a double-edged sword. Although its more porous structure tends to absorb more PBS, the lowest cross-linking density leads to an unstable architecture that is insufficient maintaining the absorbed PBS.

The disintegration behaviors of DH-G5-20%, DH-G5-Ac^{64}-20%, DH-G5-Ac^{90}-20%, and DH-G5-Ac^{106}-20% were also investigated and the results are shown in Figure 3C. All the four DHs were stable within 6 h since no more than 3% of mass loss was observed. Except for DH-G5-Ac^{106}-20%, the other three DHs could maintain their structural integrity within 24 h with no more than 6% of mass loss. DH-G5- Ac^{106}-20% experienced 60% and 64% of mass loss at 24 h and 48 h, respectively. At 48 h, DH-G5-20%, DH-G5-Ac^{64}-20%, and DH-G5-Ac^{90}-20% lost 7%, 12%, and 19% of mass, respectively. It seemed that the acetylation of G5 accelerated and aggravated the disintegration of the DHs. The weak alkaline of dendrimer and the aqueous proton buffer were the key triggers for accelerated degradation of ester bond. As dendrimer concentration was kept the same for all the DHs, the aqueous proton buffer became the dominant factor for disintegration kinetics. DH fabricated from highly acetylated G5 tended to form a loose network structure. A loose network architecture means quicker buffer absorption, which in turn, accelerates the disintegration of the hydrogel structure.

Tunable Rheological Properties

An oscillatory time sweep was performed for G5-Ac^{x}-5% and PEG-DA mixtures to monitor the evolution of storage modulus (G') and loss modulus (G''). For a typical hydrogel formulation, in the early stage, G'' is higher than G', indicating the viscous property of a sol state. When G' exceeds G'', it indicates a gel forms and the elastic property dominates. The intersection between G' and G'' reflects the sol-to-gel transition.[50–53] As shown in Figure 4A, G' is higher than G'' at the beginning and there is no intersection of G' and G''. That is presumably because the gelation occurred so quickly that the sol-to-gel transition had completed prior to the measurement. The sol-to-gel transition of DH-G5-Ac^{64}-5% and DH-G5-Ac^{90}-5% occurred at 5–7 min and 10–20 min, respectively. As for G5-Ac^{106}-5%, it did not show any obvious changes of G' and G'' within 50 min. It is worth noting that after the gelation point, G' was still increasing. That means that the gelation point shown in a time sweep only indicates an effective network forms at this point and elastic property dominates

henceforth. The formation of a completely cross-linked network would require a longer time. This explains why the gelation times obtained from the time sweep of DH-G5-5%, DH-G5-Ac^{64}-5% and DH-G5-Ac^{90}-5% were less than that observed in the invert tube method (Figure 2). However, both time sweep and inverted test tube method agreed well on that acetylation would extend the gelation time.

To further demonstrate the 3-dimensional structure of the hydrogels, the oscillatory frequency sweep was performed on all the samples. Before the frequency sweep, an amplitude sweep was carried out to make sure that the measurement was in the linear viscoelastic region (Figure S2). As shown in Figure 4B, G′ was higher than G″ for all the samples. G′ was frequency-independent over the entire measured frequency range for DH-G5-5% and DH-G5-Ac^{64}-5% and at lower frequency range for DH-G5-Ac^{90}-5% and DH-G5-Ac^{106}-5%. The frequency-independency of G′ and G′ > G″ were typically viscoelastic behavior of hydrogel.[54,55] DH-G5-5% and DH-G5-Ac^{64}-5% form stable network structures because of the high density of amine groups on the dendrimer surface. As for DH-G5-Ac^{90}-5% and DH-G5-Ac^{106}-5%, higher frequency affects their G′, further confirming their network structures are relatively less stable. G′ of DH-G5-5% (~10^3 Pa) was much higher that G′ of DH-G5-Ac^{64}-5%, DH-G5-Ac^{90}-5% and DH-G5-Ac^{106}-5% (~10^0 Pa). The highest cross-linked density of DH-G5-5% was attributed to its highest elasticity. In summary, by changing the degree of acetylation of G5, one can easily tune the cross-linking density of the DHs and modulate their gelation time and rheological properties.

Solidified Dendrimer Hydrogel Supports Cell Adhesion and Growth

To study the cell attachment and proliferation on the dendrimer hydrogel, FITC-labeled DH-G5-Ac^{64}-10% was used because of its good cytocompatility and ability to form solidified gel in situ in a short time (solidification time 38 min) for possible cell attachment. Cell culture and proliferation on TCPS was included as control. As shown in Figure 5 (middle panel), NIH3T3 cells can adhere to and grow on the hydrogel substrate. The cells were counterstained with DAPI and colocalized with FITC-stained hydrogel substrate. More cells were found at 48 h, indicating their proliferation despite at a lower rate than those on TCPS (Figure S5). The letters ‘VCU’ written using DH-G5(FITC)-Ac^{64}-10% after 24 h and 48 h incubation further confirmed the stability of this dendrimer hydrogel during the cell culture. WST-1 assay showed that the hydrogel was well tolerated by the cells and did not reduce cell viability (Figure S6). Cell attachment is attributed in large part to the positive charge, surface microstructure, and structural stability of the dendrimer hydrogel.

Liquid Dendrimer Hydrogel for Drug Delivery

DH-G5-0.5% was selected to formulate an injectable drug/hydrogel formulation for intratumoral anticancer drug delivery. The frequency sweep of DH-G5-0.5% (Figure 6A) confirmed that it formed a stable liquid hydrogel as its G′ was greater than its G″. The SEM image shown in Figure 6B illustrates its network structure. Compared to the other formulations, DH-G5-0.5% can remain its fluidity. The fluidity of the formulation makes intratumoral injection more operable. A low concentration of G5 in the formulation would avoid the risk of causing cumulative toxicity to the tissue. Cytotoxicity study revealed that DH-G5-0.5% is highly cytocompatible. It did not cause toxicity effects up to 50 mg/mL

(equivalent to 250 μg/mL of G5) following 24-h or 48 h-exposure (Figure 6C). When the concentration was doubled, only less than of 20% reduce in cell viability was observed. 5-FU can be slowly released from DH-G5-0.5% (Figure 6D). An initial burst release followed by sustained release was observed for both 5-FU/PBS and 5-FU/DH-G5-0.5%. However, DH-G5-0.5% extended the duration of both burst release and sustained release. Nearly 70% of 5-FU was released within just 0.5 h from the PBS control group and then quickly reached a plateau of 80% in 2 h. In contrast, the release of 5-FU from DH-G5-0.5% was prolonged. About 60% of 5-FU was released from DH-G5-0.5% within 1 h and a longer time (6 h) was spent before the cumulative release plateau of 80% was reached. In the formulation of 5-FU/DH-G5-0.5%, part of 5-FU was complexed with dendrimers via electrostatic and hydrophobic interactions, whereas the rest of 5-FU was loosely entrapped in the hydrogel network. The burst release within 1 h was due to the release of 5-FU in the gel network. The following sustained release was caused by the diffusion of 5-FU from the interior of dendrimer. The release test demonstrated that such a low viscous liquid hydrogel is still capable of slowly releasing drug. The injectability, biocompatibility and sustained drug release made DH-G5-0.5% a suitable formulation for intratumoral drug delivery test.

Solid tumors such as head and neck cancer are accessible and can benefit from localized chemotherapy for stronger antitumor effects and less systemic toxicity. We tested this new drug formulation in a head and neck cancer model via intratumoral injection and compared it with 5-FU/PBS. 5-FU/PBS did not show significant tumor inhibition effects. In contrast, 5-FU/DH-G5-0.5% shows a strong trend inhibiting tumor growth (Figure 7A). The tumor volume became significantly lower than the rest treatment groups at day 17. Compared to the terminal tumor volume of the PBS group, 5-FU/DH-G5-0.5% reduced tumor volume by 4 folds, indicating that the drug/dendrimer hydrogel formulation promoted significantly better *in vivo* anticancer efficacy. The body weight of the tumor-bearing mice was also monitored. There was no obvious loss of body weight for the mice during the treatment (Figure 7B). The end-point tumor images (Figure 7C) further illustrate the significantly reduced tumor size by 5-FU/DH-G5-0.5%. H&E staining (Figure 7D) shows that 5-FU/DH-G5-0.5% resulted in high massive tumor cell remission. Furthermore, the H& E staining did not reveal any morphological change in the blank hydrogel group, indicating the nontoxicity of the hydrogel itself. Taken together, injectable dendrimer hydrogel provides a sustained drug delivery platform for localized chemotherapy.

CONCLUSIONS

A novel type of PAMAM dendrimer hydrogel was successfully developed based on aza-Michael addition chemistry. The solidification time, rheological behavior, network structure and swelling property of the hydrogel can be modulated by adjusting dendrimer surface acetylation degree and dendrimer concentration. In addition, the new PAMAM dendrimer hydrogels have good biocompatibility and support cell adhesion and proliferation. The dendrimer hydrogel can be utilized to prepare injectable drug formulations for localized chemotherapy. This hydrogel with tunable properties prepared by aza-Michael addition reaction can serve as a new platform for drug delivery and tissue engineering.

Supplementary Material

Refer to Web version on PubMed Central for supplementary material.

Acknowledgments

The authors thank Dr. Christina Tang (Department of Chemical and Life Science Engineering, Virginia Commonwealth University) for the use of Discovery hybrid rheometer HR-3. Dr. Leyuan Xu provided advice on acetylation and drug release experiments. This work was supported, in part, by the National Science Foundation (CAREER award CBET0954957), and National Institutes of Health (R01EY024072).

References

1. Yu L, Ding J. Injectable Hydrogels as Unique Biomedical Materials. Chem Soc Rev. 2008; 37:1473–1481. [PubMed: 18648673]
2. Bae KH, Wang LS, Kurisawa M. Injectable Biodegradable Hydrogels: Progress and Challenges. J Mater Chem B. 2013; 1:5371–5388.
3. Li Y, Rodrigues J, Tomas H. Injectable and Biodegradable Hydrogels: Gelation, Biodegradation and Biomedical Applications. Chem Soc Rev. 2012; 41:2193–2221. [PubMed: 22116474]
4. Purcell BP, Lobb D, Charati MB, Dorsey SM, Wade RJ, Zellers KN, Doviak H, Pettaway S, Logdon CB, Shuman J, Freels PD, Gorman JH, Gorman RC, Spinale FG, Burdick JA. Injectable and Bioresponsive Hydrogels for On-Demand Matrix Metalloproteinase Inhibition. Nature Mater. 2014; 13:653–661. [PubMed: 24681647]
5. Nguyen QV, Huynh DP, Park JH, Lee DS. Injectable Polymeric Hydrogels for the Delivery of Therapeutic Agents: A Review. Eur Polym J. 2015; 72:602–619.
6. Ruel-Gariépy E, Leroux JC. In Situ-Forming Hydrogels—Review of Temperature-Sensitive Systems. Eur J Pharm Biopharm. 2004; 58:409–426. [PubMed: 15296964]
7. Kim DY, Kwon DY, Kwon JS, Park JH, Park SH, Oh HJ, Kim JH, Min BH, Park K, Kim MS. Synergistic Anti-Tumor Activity through Combinational Intratumoral Injection of An In-Situ Injectable Drug Depot. Biomaterials. 2016; 85:232–245. [PubMed: 26874285]
8. Wang C, Wang X, Dong K, Luo J, Zhang Q, Cheng Y. Injectable and Responsively Degradable Hydrogel for Personalized Photothermal Therapy. Biomaterials. 2016; 104:129–137. [PubMed: 27449949]
9. Fakhari A, Anand Subramony J. Engineered In-Situ Depot-Forming Hydrogels for Intratumoral Drug Delivery. J Control Release. 2015; 220:465–475. [PubMed: 26585504]
10. Gao W, Liang Y, Peng X, Hu Y, Zhang L, Wu H, He B. In Situ Injection of Phenylboronic Acid Based Low Molecular Weight Gels for Efficient Chemotherapy. Biomaterials. 2016; 105:1–11. [PubMed: 27497056]
11. Lammers T, Peschke P, Kühnlein R, Subr V, Ulbrich K, Huber P, Hennink W, Stormy G. Effect of Intratumoral Injection on the Biodistribution and the Therapeutic Potential of HPMA Copolymer-Based Drug Delivery Systems. Neoplasia. 2006; 8:788–795. [PubMed: 17032495]
12. Li L, Gu J, Zhang J, Xie Z, Lu Y, Shen L, Dong Q, Wang Y. Injectable and Biodegradable pH-Responsive Hydrogels for Localized and Sustained Treatment of Human Fibrosarcoma. ACS Appl Mater Interfaces. 2015; 7:8033–8040. [PubMed: 25838258]
13. Xu Y, Asghar S, Li H, Chen M, Su Z, Xu Y, Ping Q, Xiao Y. Preparation of A Paclitaxel-Loaded Cationic Nanoemulsome and Its Biodistribution via Direct Intratumoral Injection. Colloids Surf, B. 2016; 142:81–88.
14. Custódio CA, Reis RL, Mano JF. Photo-Cross-Linked Laminarin-Based Hydrogels for Biomedical Applications. Biomacromolecules. 2016; 17:1602–1609. [PubMed: 27017983]
15. Yue K, Trujillo-de Santiago G, Alvarez MM, Tamayol A, Annabi N, Khademhosseini A. Synthesis, Properties, and Biomedical Applications of Gelatin Methacryloyl (GelMA) Hydrogels. Biomaterials. 2015; 73:254–271. [PubMed: 26414409]

16. Ghobril C, Charoen K, Rodriguez EK, Nazarian A, Grinstaff MW. A Dendritic Thioester Hydrogel Based on Thiol–Thioester Exchange as A Dissolvable Sealant System for Wound Closure. Angew Chem, Int Ed. 2013; 52:14070–14074.
17. Higginson CJ, Kim SY, Peláez-Fernández M, Fernández-Nieves A, Finn MG. Modular Degradable Hydrogels Based on Thiol-Reactive Oxanorbornadiene Linkers. J Am Chem Soc. 2015; 137:4984–4987. [PubMed: 25871459]
18. Jee E, Bánsági T, Taylor AF, Pojman JA. Temporal Control of Gelation and Polymerization Fronts Driven by An Autocatalytic Enzyme Reaction. Angew Chem, Int Ed. 2016; 128:2167–2171.
19. Liu ZQ, Wei Z, Zhu XL, Huang GY, Xu F, Yang JH, Osada Y, Zrínyi M, Li JH, Chen YM. Dextran-Based Hydrogel Formed by Thiol-Michael Addition Reaction for 3D Cell Encapsulation. Colloids Surf, B. 2015; 128:140–148.
20. Xu G, Wang X, Deng C, Teng X, Suuronen EJ, Shen Z, Zhong Z. Injectable Biodegradable Hybrid Hydrogels Based on Thiolated Collagen and Oligo(acryloyl carbonate)–poly(ethylene glycol)–oligo(acryloyl carbonate) Copolymer for Functional Cardiac Regeneration. Acta Biomater. 2015; 15:55–64. [PubMed: 25545323]
21. Balakrishnan B, Jayakrishnan A. Self-Cross-Linking Biopolymers as Injectable In Situ Forming Biodegradable Scaffolds. Biomaterials. 2005; 26:3941–3951. [PubMed: 15626441]
22. Martínez-Sanz E, Ossipov DA, Hilborn J, Larsson S, Jonsson KB, Varghese OP. Bone Reservoir: Injectable Hyaluronic Acid Hydrogel for Minimal Invasive Bone Augmentation. J Control Release. 2011; 152:232–240. [PubMed: 21315118]
23. Xin Y, Yuan J. Schiff's Base as A Stimuli-Responsive Linker in Polymer Chemistry. Polym Chem. 2012; 3:3045–3055.
24. Chen F, Yu S, Liu B, Ni Y, Yu C, Su Y, Zhu X, Yu X, Zhou Y, Yan D. An Injectable Enzymatically Crosslinked Carboxymethylated Pullulan/Chondroitin Sulfate Hydrogel for Cartilage Tissue Engineering. Sci Rep. 2016; 6:20014. [PubMed: 26817622]
25. Jin R, Hiemstra C, Zhong Z, Feijen J. Enzyme-Mediated Fast In Situ Formation of Hydrogels from Dextran–Tyramine Conjugates. Biomaterials. 2007; 28:2791–2800. [PubMed: 17379300]
26. Sakai S, Hirose K, Taguchi K, Ogushi Y, Kawakami K. An Injectable, In Situ Enzymatically Gellable, Gelatin Derivative for Drug Delivery and Tissue Engineering. Biomaterials. 2009; 30:3371–3377. [PubMed: 19345991]
27. Sakai S, Yamada Y, Zenke T, Kawakami K. Novel Chitosan Derivative Soluble at Neutral pH and In-Situ Gellable via Peroxidase-Catalyzed Enzymatic Reaction. J Mater Chem. 2009; 19:230–235.
28. Roy D, Brooks WLA, Sumerlin BS. New Directions in Thermoresponsive Polymers. Chem Soc Rev. 2013; 42:7214–7243. [PubMed: 23450220]
29. Bakota EL, Wang Y, Danesh FR, Hartgerink JD. Injectable Multidomain Peptide Nanofiber Hydrogel as A Delivery Agent for Stem Cell Secretome. Biomacromolecules. 2011; 12:1651–1657. [PubMed: 21417437]
30. Park H, Woo EK, Lee KY. Ionically Cross-Linkable Hyaluronate-Based Hydrogels for Injectable Cell Delivery. J Control Release. 2014; 196:146–153. [PubMed: 25315489]
31. Wang D, Wagner M, Butt HJ, Wu S. Supramolecular Hydrogels Constructed by Red-Light-Responsive Host–Guest Interactions for Photo-Controlled Protein Release in Deep Tissue. Soft Matter. 2015; 11:7656–7662. [PubMed: 26292617]
32. Ma D, Tu K, Zhang LM. Bioactive Supramolecular Hydrogel with Controlled Dual Drug Release Characteristics. Biomacromolecules. 2010; 11:2204–2212. [PubMed: 20831271]
33. Ghobril C, Rodriguez EK, Nazarian A, Grinstaff MW. Recent Advances in Dendritic Macromonomers for Hydrogel Formation and Their Medical Applications. Biomacromolecules. 2016; 17:1235–1252. [PubMed: 26978246]
34. Konieczynska MD, Villa-Camacho JC, Ghobril C, Perez-Viloria M, Tevis KM, Blessing WA, Nazarian A, Rodriguez EK, Grinstaff MW. On-Demand Dissolution of A Dendritic Hydrogel-Based Dressing for Second-Degree Burn Wounds through Thiol–Thioester Exchange Reaction. Angew Chem, Int Ed. 2016; 55:9984–9987.
35. Oelker AM, Berlin JA, Wathier M, Grinstaff MW. Synthesis and Characterization of Dendron Cross-Linked PEG Hydrogels as Corneal Adhesives. Biomacromolecules. 2011; 12:1658–1665. [PubMed: 21417379]

36. Wang Y, Zhao Q, Luo Y, Xu Z, Zhang H, Yang S, Wei Y, Jia X. A High Stiffness Bio-Inspired Hydrogel from the Combination of A Poly(amido amine) Dendrimer with DOPA. Chem Commun. 2015; 51:16786–16789.
37. Wang Y, Zhao Q, Zhang H, Yang S, Jia X. A Novel Poly(amido amine)-Dendrimer-Based Hydrogel as A Mimic for the Extracellular Matrix. Adv Mater. 2014; 26:4163–4167. [PubMed: 24729192]
38. Zhang H, Patel A, Gaharwar AK, Mihaila SM, Iviglia G, Mukundan S, Bae H, Yang H, Khademhosseini A. Hyperbranched Polyester Hydrogels with Controlled Drug Release and Cell Adhesion Properties. Biomacromolecules. 2013; 14:1299–1310. [PubMed: 23394067]
39. Zhou F, Chen L, An Q, Chen L, Wen Y, Fang F, Zhu W, Yi T. Novel Hydrogel Material as A Potential Embolic Agent in Embolization Treatments. Sci Rep. 2016; 6:32145. [PubMed: 27561915]
40. Desai PN, Yuan Q, Yang H. Synthesis and Characterization of Photocurable Polyamidoamine Dendrimer Hydrogels as A Versatile Platform for Tissue Engineering and Drug Delivery. Biomacromolecules. 2010; 11:666–673. [PubMed: 20108892]
41. Holden CA, Tyagi P, Thakur A, Kadam R, Jadhav G, Kompella UB, Yang H. Polyamidoamine Dendrimer Hydrogel for Enhanced Delivery of Antiglaucoma Drugs. Nanomedicine. 2012; 8:776–83. [PubMed: 21930109]
42. Navath RS, Menjoge AR, Wang B, Romero R, Kannan S, Kannan RM. Amino Acid-Functionalized Dendrimers with Heterobifunctional Chemoselective Peripheral Groups for Drug Delivery Applications. Biomacromolecules. 2010; 11:1544–1563. [PubMed: 20415504]
43. Shen Y, Zhang S, Wan Y, Fu W, Li Z. Hydrogels Assembled from Star-Shaped Polypeptides with A Dendrimer as the Core. Soft Matter. 2015; 11:2945–2951. [PubMed: 25720319]
44. Yang H, Tyagi P, Kadam RS, Holden CA, Kompella UB. Hybrid Dendrimer Hydrogel/PLGA Nanoparticle Platform Sustains Drug Delivery for One Week and Antiglaucoma Effects for Four Days Following One-Time Topical Administration. ACS Nano. 2012; 6:7595–7606. [PubMed: 22876910]
45. Majoros IJ, Myc A, Thomas T, Mehta CB, Baker JR. PAMAM Dendrimer-Based Multifunctional Conjugate for Cancer Therapy: Synthesis, Characterization, and Functionality. Biomacromolecules. 2006; 7:572–579. [PubMed: 16471932]
46. Myc A, Majoros IJ, Thomas TP, Baker JR. Dendrimer-Based Targeted Delivery of An Apoptotic Sensor in Cancer Cells. Biomacromolecules. 2007; 8:13–18. [PubMed: 17206782]
47. Xu LY, Zolotarskaya OY, Yeudall WA, Yang H. Click Hybridization of Immune Cells and Polyamidoamine Dendrimers. Adv Healthcare Mater. 2014; 3:1430–1438.
48. Wu DC, Liu Y, He CB, Chung TS, Goh ST. Effects of Chemistries of Trifunctional Amines on Mechanisms of Michael Addition Polymerizations with Diacrylates. Macromolecules. 2004; 37:6763–6770.
49. Zeng Y, Kurokawa Y, Win-Shwe TT, Zeng Q, Hirano S, Zhang Z, Sone H. Effects of PAMAM Dendrimers with Various Surface Functional Groups and Multiple Generations on Cytotoxicity and Neuronal Differentiation Using Human Neural Progenitor Cells. J Toxicol Sci. 2016; 41:351–370. [PubMed: 27193728]
50. Balakrishnan B, Joshi N, Jayakrishnan A, Banerjee R. Self-Crosslinked Oxidized Alginate/Gelatin Hydrogel as Injectable, Adhesive Biomimetic Scaffolds for Cartilage Regeneration. Acta biomater. 2014; 10:3650–3663. [PubMed: 24811827]
51. Ghosh K, Shu XZ, Mou R, Lombardi J, Prestwich GD, Rafailovich MH, Clark RAF. Rheological Characterization of In Situ Cross-Linkable Hyaluronan Hydrogels. Biomacromolecules. 2005; 6:2857–2865. [PubMed: 16153128]
52. Rudraraju VS, Wyandt CM. Rheology of Microcrystalline Cellulose and Sodiumcarboxymethyl Cellulose Hydrogels Using A Controlled Stress Rheometer: Part II. Int J Pharm. 2005; 292:63–73. [PubMed: 15725554]
53. Zuidema JM, Rivet CJ, Gilbert RJ, Morrison FA. A Protocol for Rheological Characterization of Hydrogels for Tissue Engineering Strategies. J Biomed Mater Res, Part B. 2014; 102:1063–1073.

54. Higham AK, Garber LA, Latshaw DC, Hall CK, Pojman JA, Khan SA. Gelation and Cross-Linking in Multifunctional Thiol and Multifunctional Acrylate Systems Involving An In Situ Comonomer Catalyst. Macromolecules. 2014; 47:821–829.

55. Wu J, Liu J, Shi Y, Wan Y. Rheological, Mechanical and Degradable Properties of Injectable Chitosan/Silk Fibroin/Hydroxyapatite/Glycerophosphate Hydrogels. J Mech Behav Biomed Mater. 2016; 64:161–172. [PubMed: 27498426]

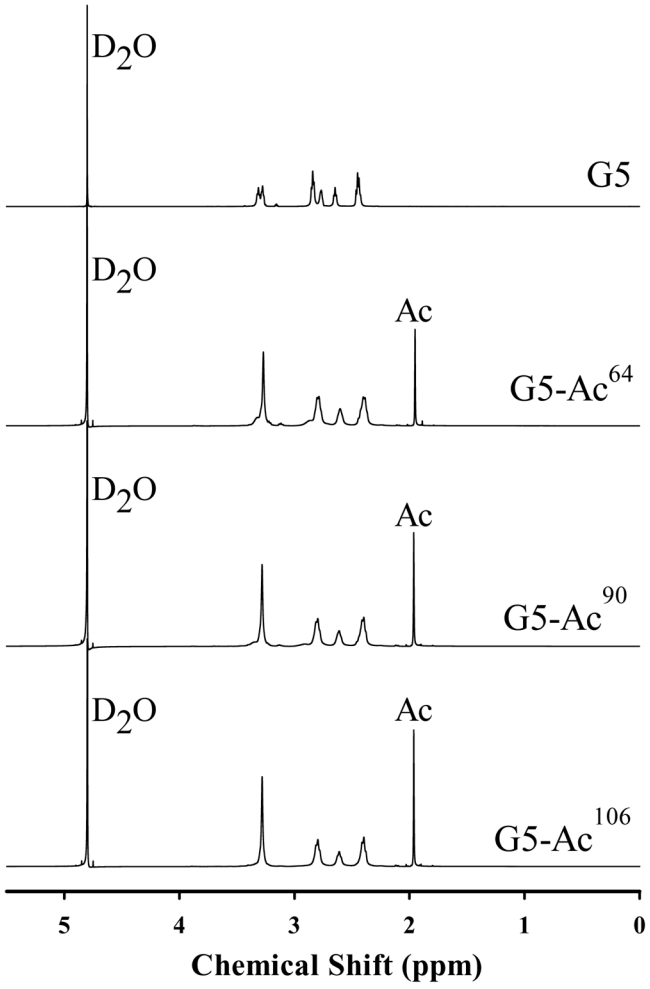

A

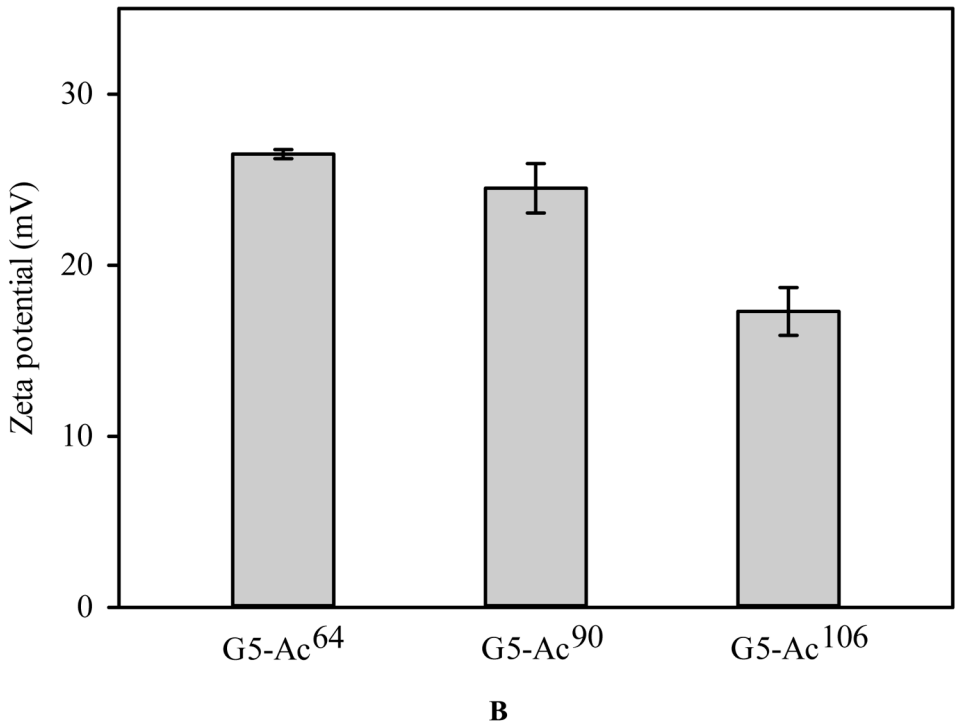

FIGURE 1.
Characterization of acetylated G5. (A) ^{1}H NMR spectra. (B) Zeta potential.

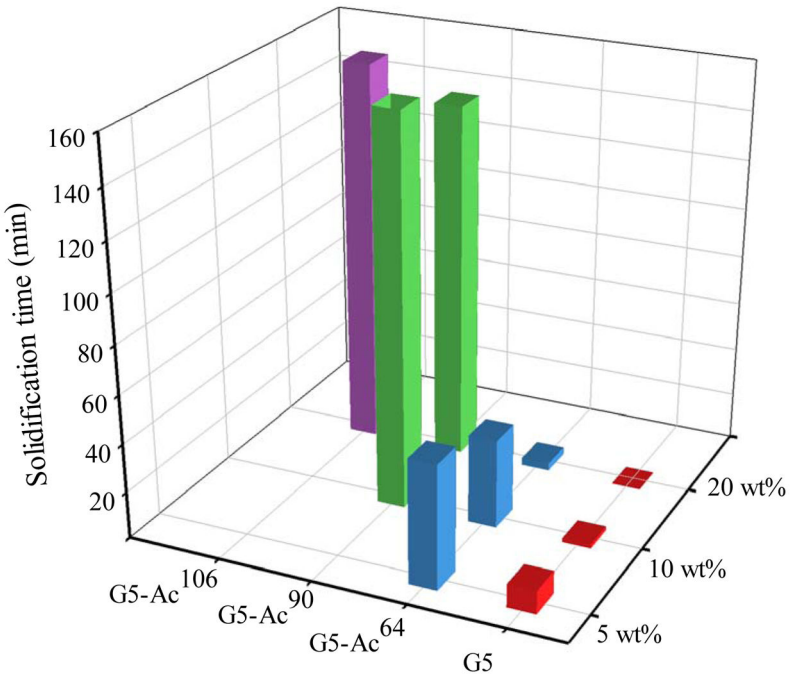

FIGURE 2.
Solidification kinetics of dendrimer hydrogels as a function of degree of acetylation and dendrimer concentration.

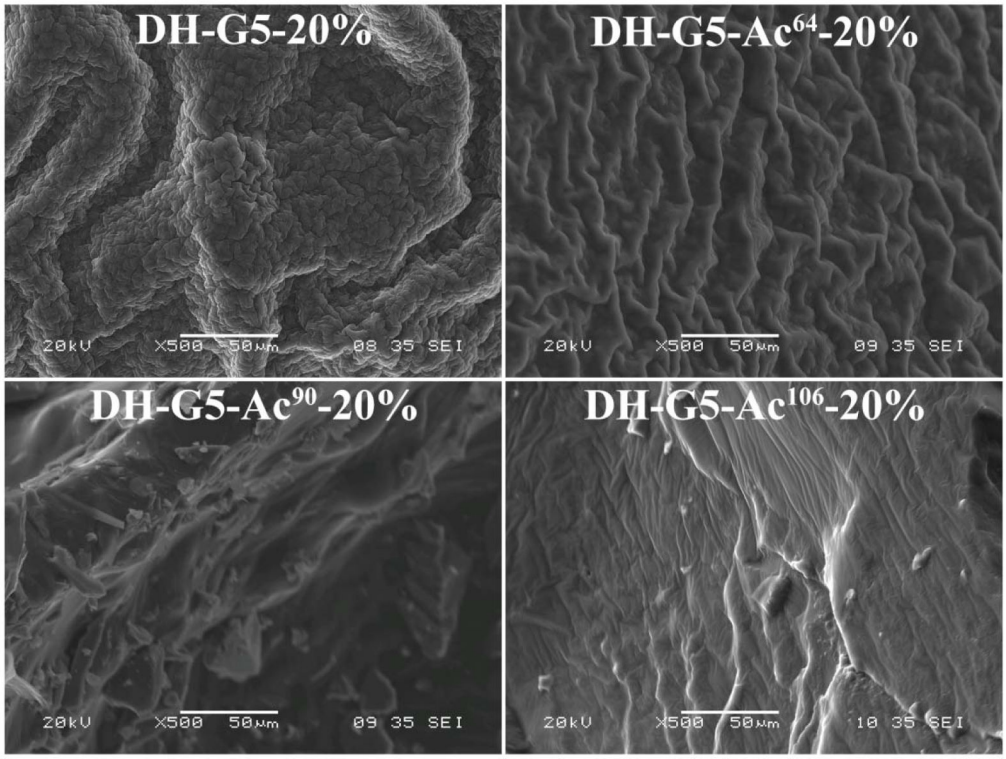

A

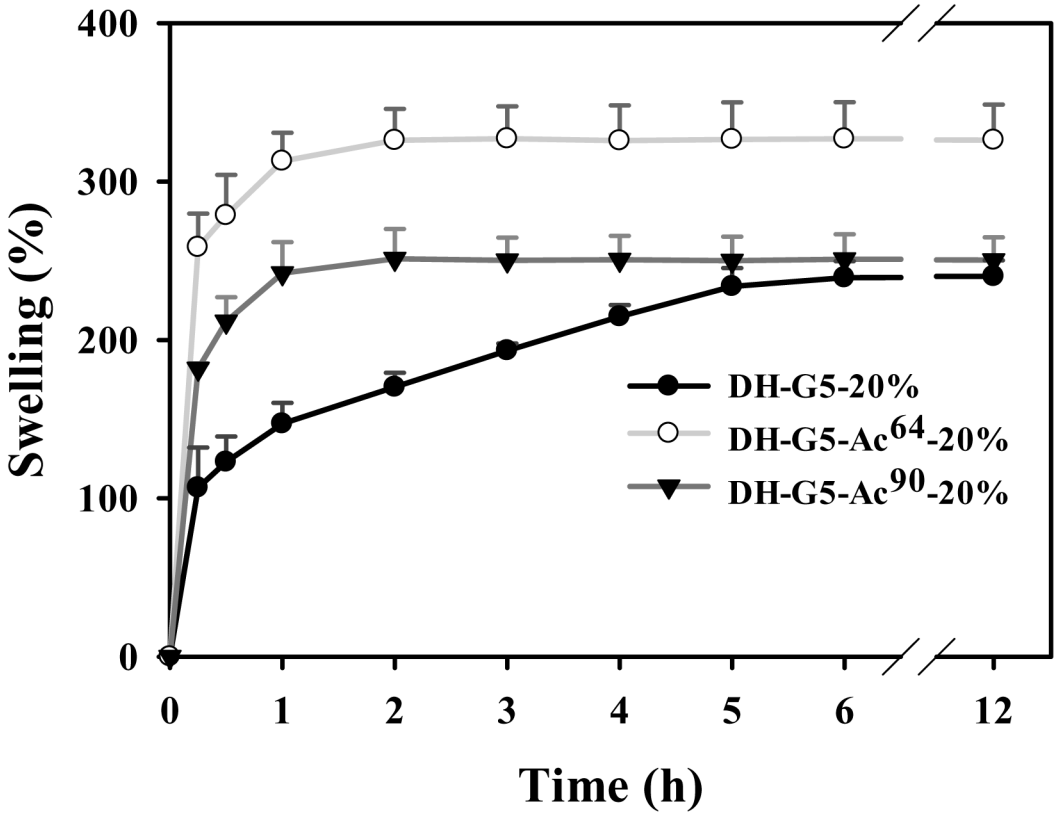

B

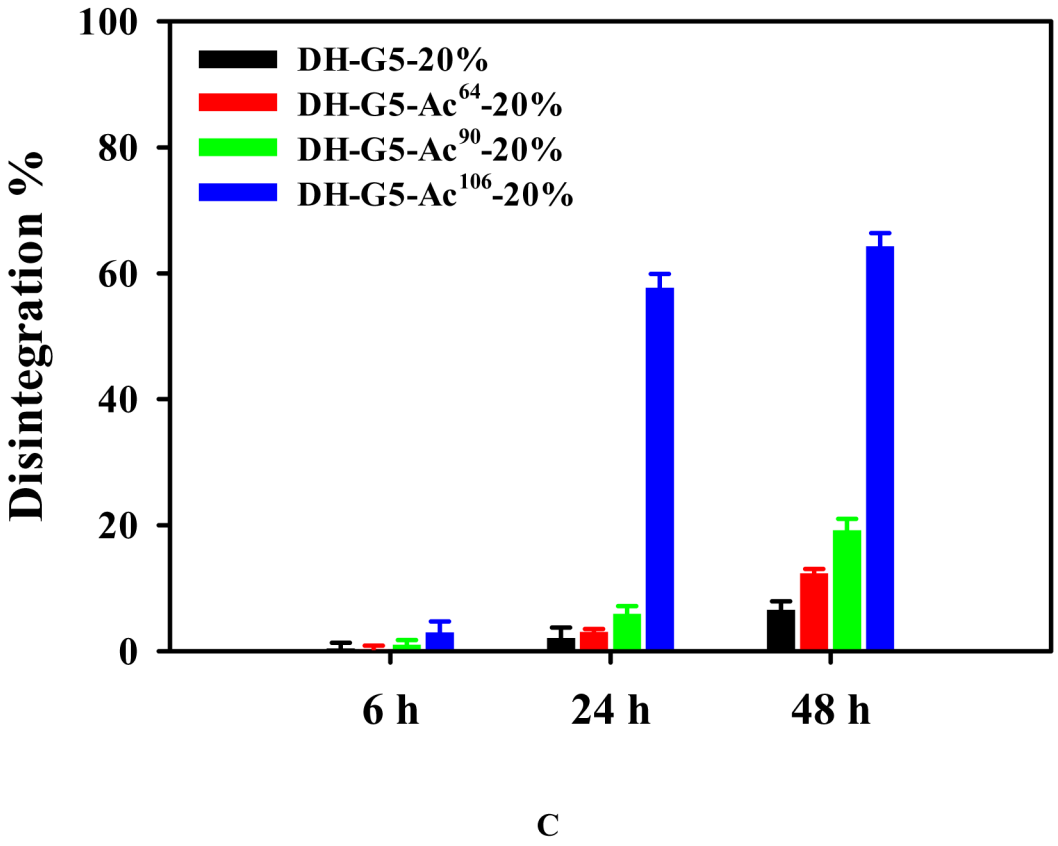

FIGURE 3.

Effects of acetylation on morphologies and swelling of dendrimer hydrogels. (A) SEM micrographs. (B) Swelling kinetics in pH 7.4 PBS at 37 °C. (C) Disintegration in pH 7.4 PBS at 37 °C.

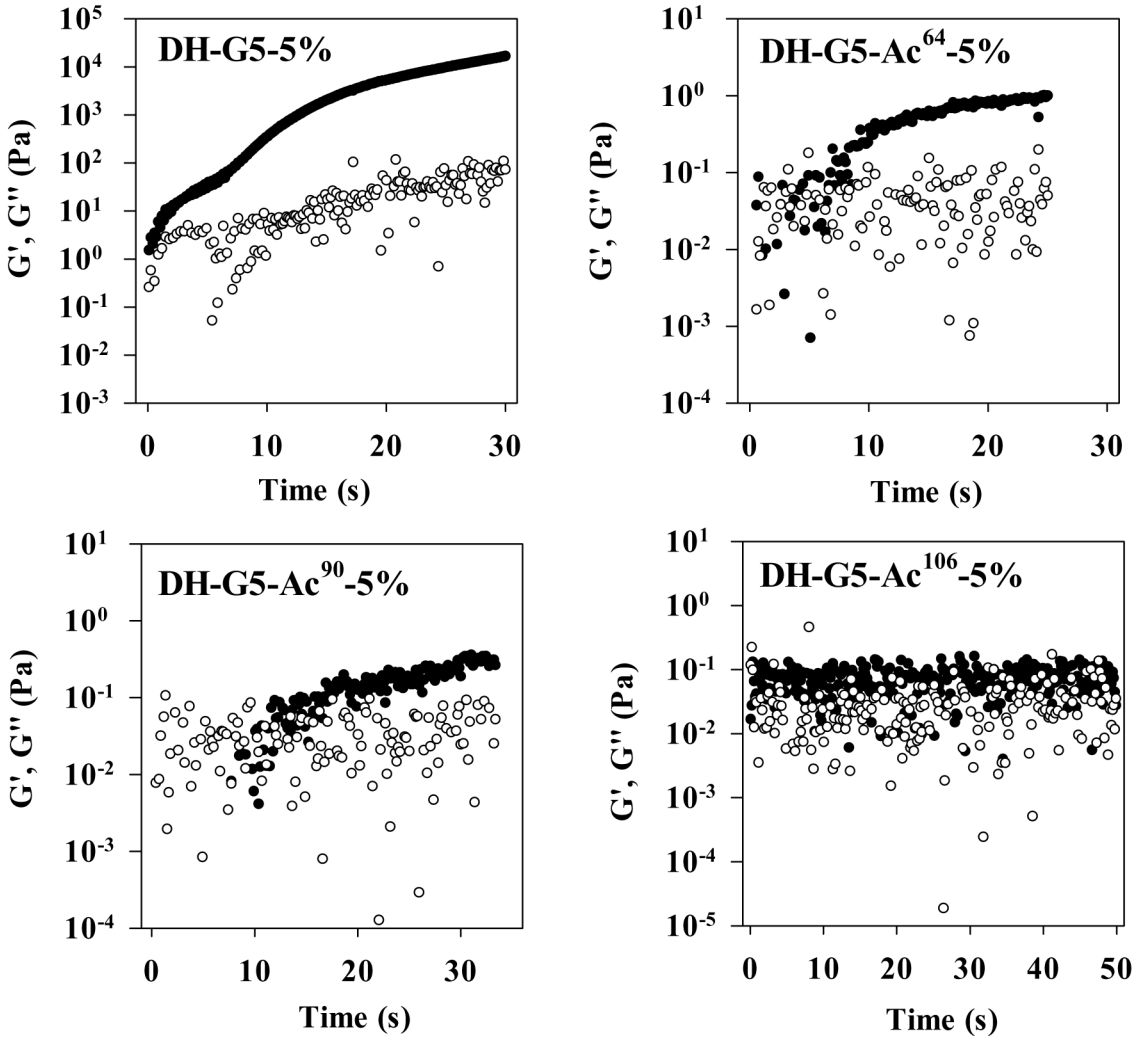

A

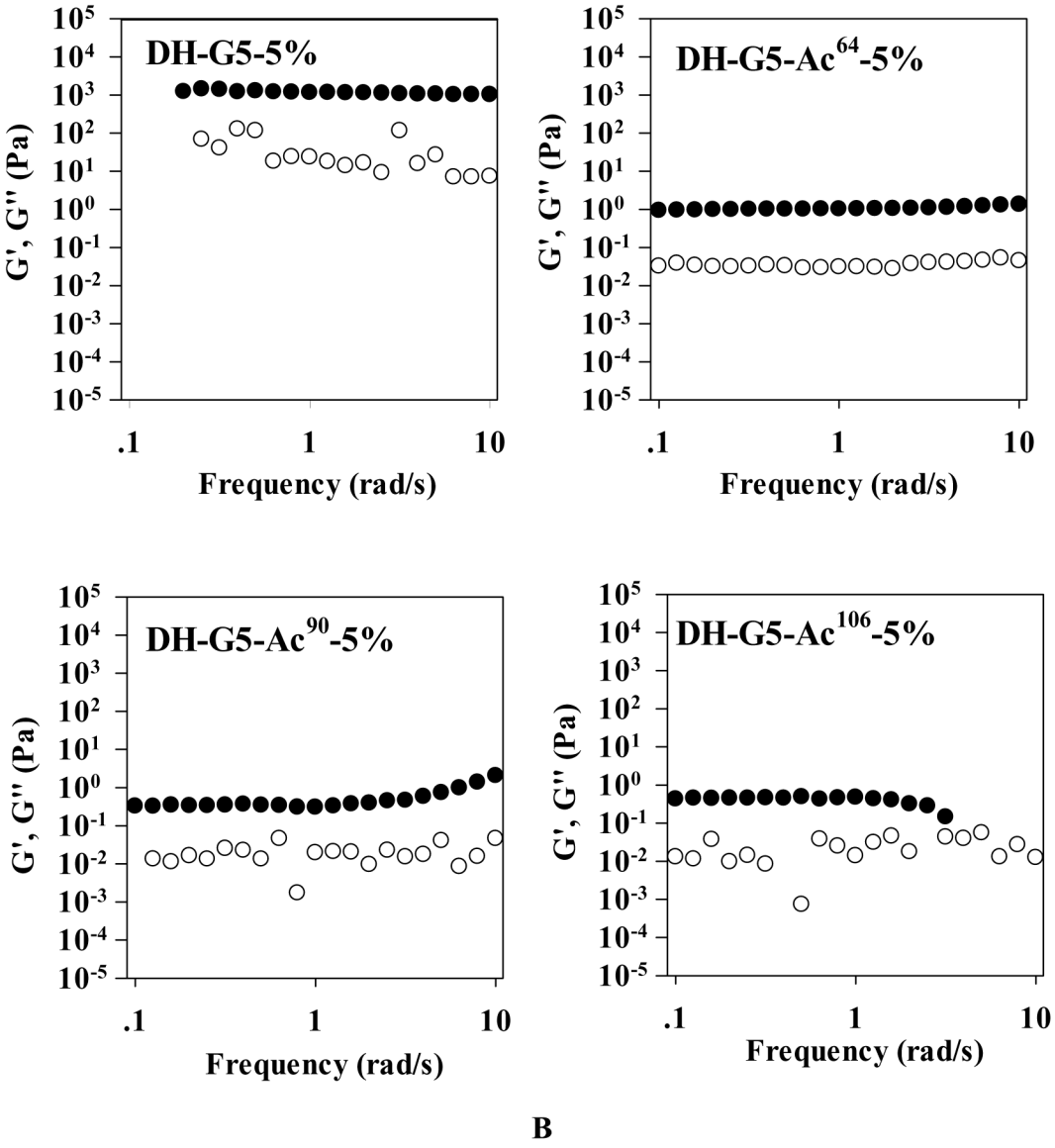

FIGURE 4.

Rheological properties of dendrimer hydrogels. (A) Oscillatory time sweep. (B) Oscillatory frequency sweep. ● represents storage modulus (G′) and ○ represents loss modulus (G″).

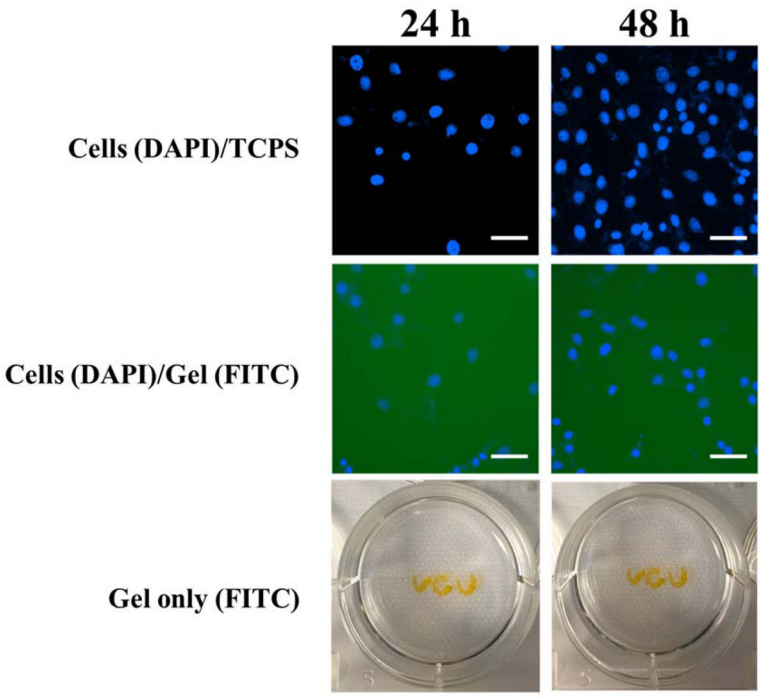

FIGURE 5.

Solidified dendrimer hydrogel supports cell adherence and proliferation. Top panel: NIH3T3 cells were directly cultured on tissue culture polystyrene plate (TCPS) for 24 h and 48 h, respectively. Middle panel: NIH3T3 cells were cultured on FITC-labeled DH-G5-Ac^{64}-10% (gel/FITC) for 24 h and 48 h, respectively. Bottom panel: The letters written with FITC-labeled DH-G5-Ac^{64}-10% and incubated in cell culture medium for 24 h and 48 h, respectively. NIH3T3 cells were counterstained with DAPI (blue). Scale bar: 100 μm.

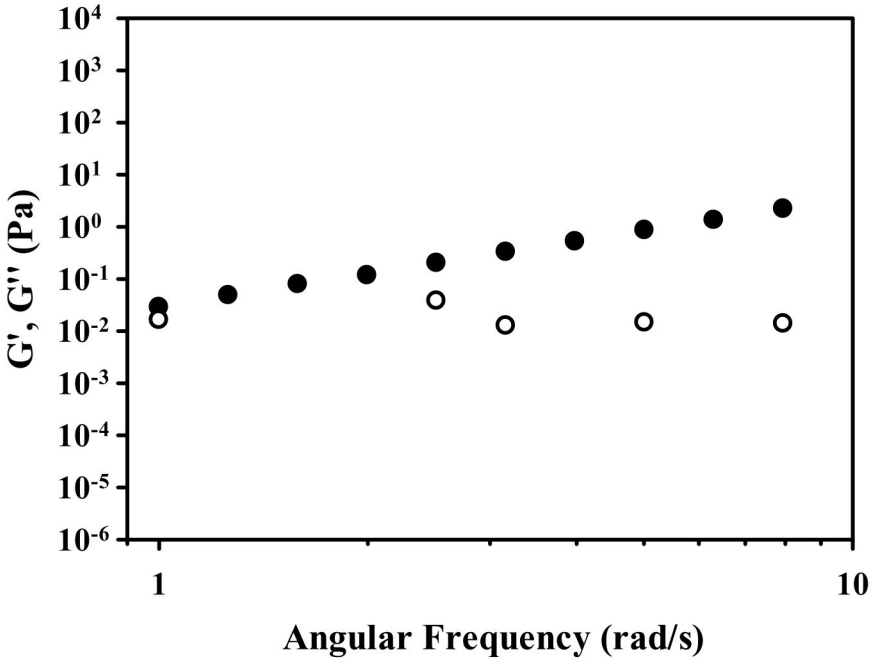

A

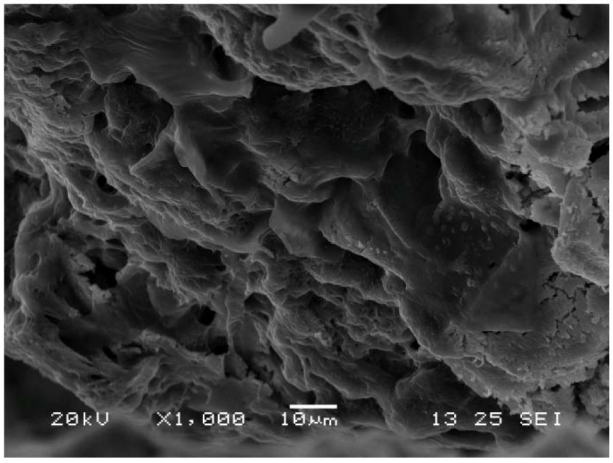

B

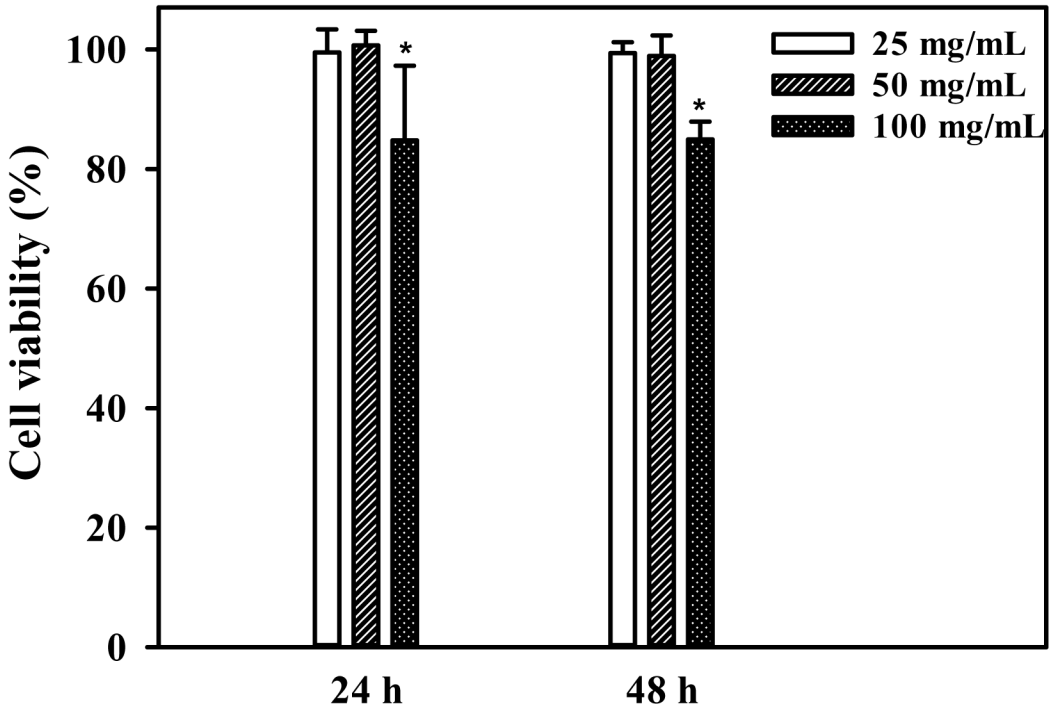

C

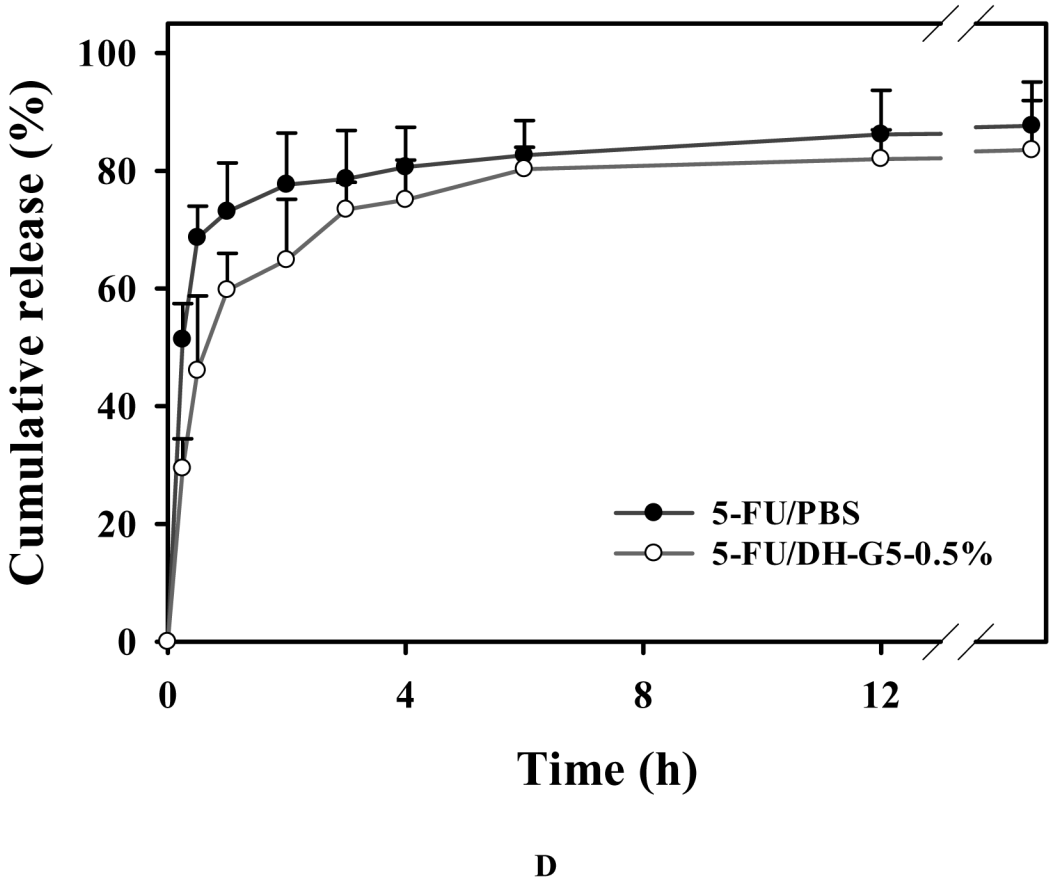

D

FIGURE 6.

Characterization and *in vitro* assessment of liquid dendrimer hydrogel DH-G5-0.5% for drug delivery. (A) Oscillatory frequency sweep of DH-G5-0.5%. ● represents storage modulus (G′) and ○ presents loss modulus (G″). (B) SEM micrograph of DH-G5-0.5%. (C) Cumulative release of 5-FU from DH-G5-0.5% in PBS buffer pH = 7.4 (n = 3) at 37 °C. (D) Cytotoxicity assay of DH-G5-0.5% (n = 6). * Statistically significant.

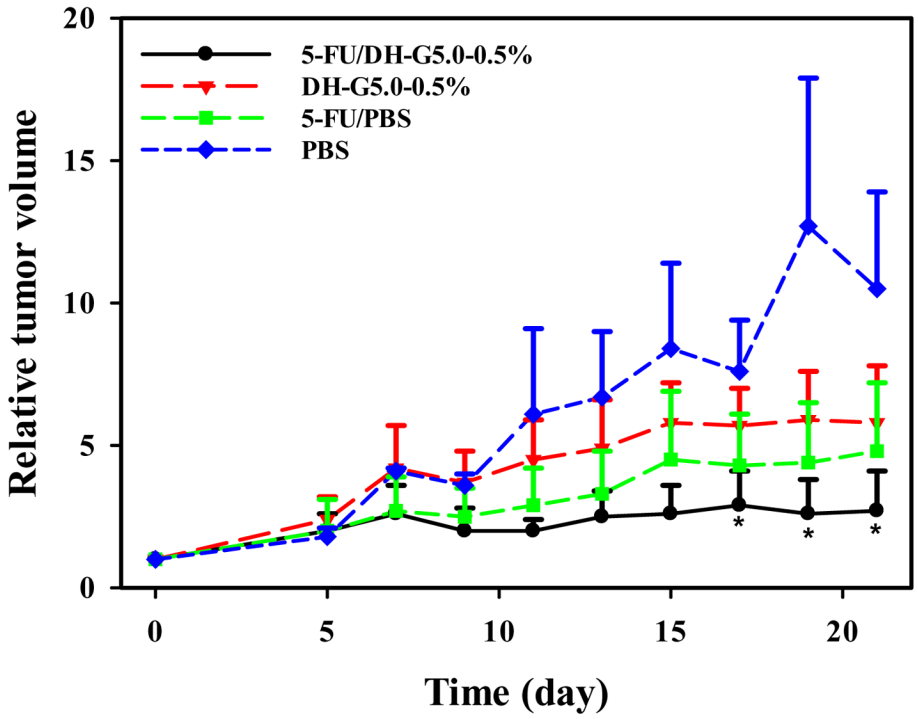

A

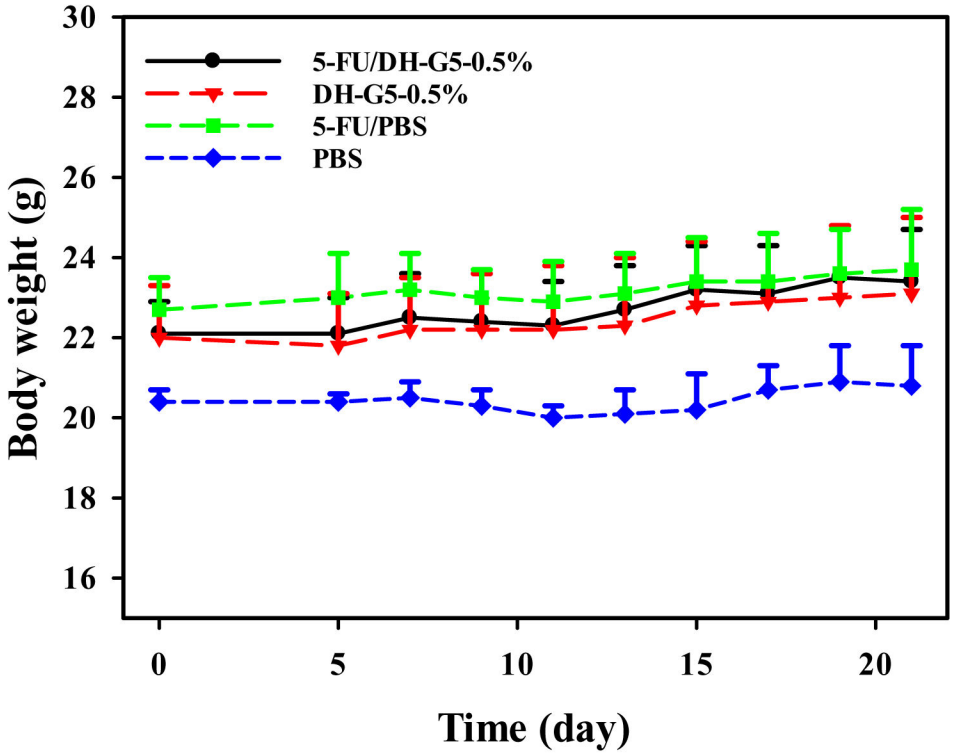

B

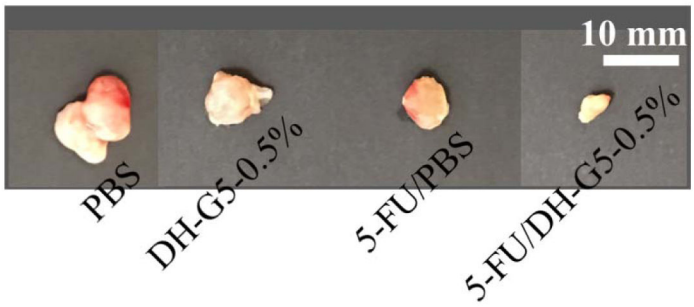

C

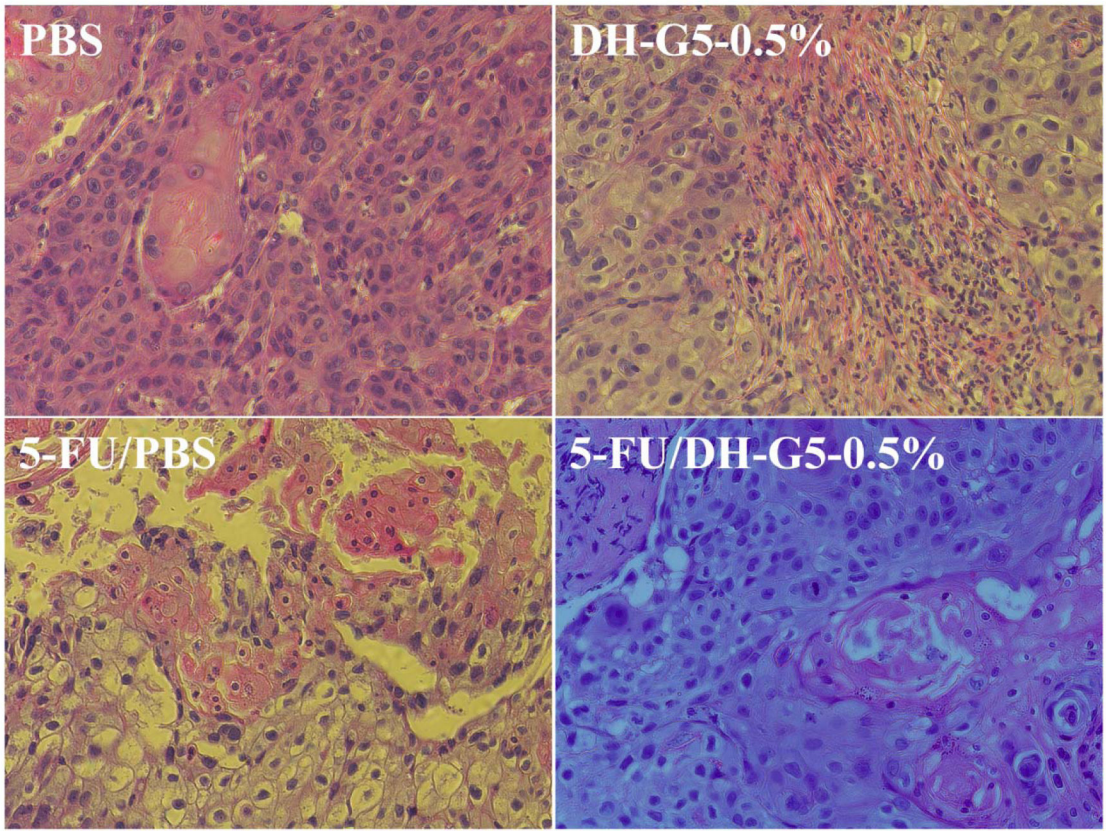

D

FIGURE 7.

In vivo antitumor assessment of 5-FU/DH-G5-0.5%. (A) Relative tumor volume change during the treatment. (B) Mice body weight change during the treatment. (C) Images of extracted tumors after the treatment. (D) H&E staining of tumor tissues after the treatment (magnification 200×). * Statistically significant.

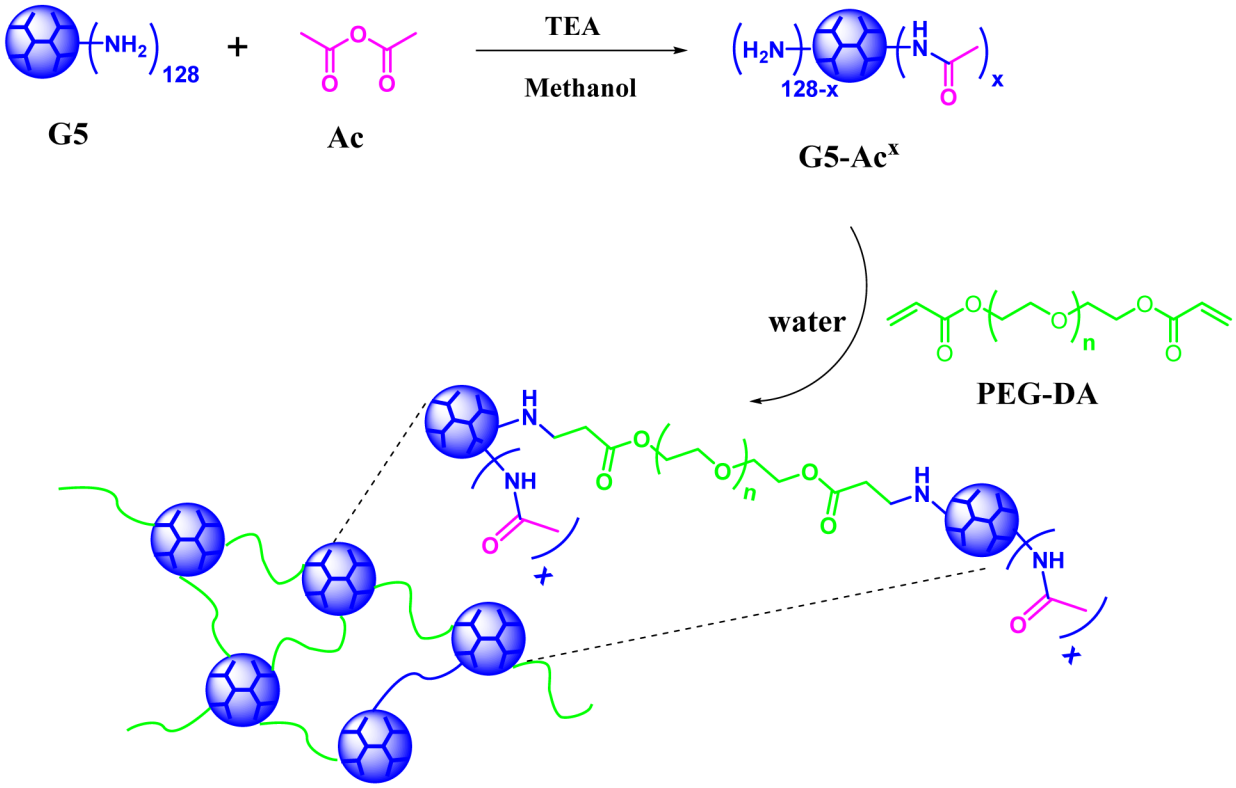

SCHEME 1.

Scheme of acetylated G5 (G%-Ac) synthesis and aza-Michael addition reaction of G5 or G5-Ac with PEG DA.

Table 1

Reaction Conditions for Synthesis of Acetylated G5.

G5-Ac^{x}[a]	molar quantities of reactants (mmol)		
	G5	Ac	TEA
G5-Ac^{64}	0.01 (1 equiv.)	0.70 (70 equiv.)	0.88 (88 equiv.)
G5-Ac^{90}	0.01 (1 equiv.)	0.97 (97 equiv.)	1.22 (122 equiv.)
G5-Ac^{106}	0.01 (1 equiv.)	1.13 (113 equiv.)	1.41 (141 equiv.)

[a] Determined by ^{1}H NMR spectroscopy.